RNA (1997), 3:464-475. Cambridge University Press. Printed in the USA.

The path of mRNA through the bacterial ribosome: A site-directed crosslinking study using new photoreactive derivatives of guanosine and uridine

PETR V. SERGIEV,[1] INNA N. LAVRIK,[1] VYACHESLAV A. WLASOFF,[1] SVETLANA S. DOKUDOVSKAYA,[1] OLGA A. DONTSOVA,[1] ALEXEY A. BOGDANOV,[1] and RICHARD BRIMACOMBE[2]

[1]Department of Chemistry, Moscow State University, 119899 Moscow, Russia
[2]Max-Planck-Institut für Molekulare Genetik, Ihnestrasse 73, 14195 Berlin, Germany

ABSTRACT

Two new photoreactive nucleotide derivatives have been applied in site-directed crosslinking studies with mRNA analogues. 6-Thioguanosine triphosphate or 5-methyleneaminouridine triphosphate was incorporated into mRNA analogues by T7 transcription; after transcription, the 5-methyleneaminouridine residues were converted to a diazirine derivative. mRNA analogues carrying either 6-thioguanosine or the diazirine derivative were bound to *Escherichia coli* ribosomes in the presence of $tRNA_f^{Met}$, and photo-crosslinking was induced by irradiation at 350 nm. With 6-thioguanosine, specific crosslinks were observed from downstream positions +8 or +9 of the mRNA to nt 1196 in helix 34 of the 16S rRNA, and from position +12 to nt 530 in helix 18. With the diazirine derivative, a crosslink from position +2 (within the AUG codon) to nt 926 in helix 28 was found. Taken together with previous data obtained from downstream sites in mRNA analogues carrying 4-thiouridine residues, specific crosslinks have now been identified from downstream mRNA positions +2, +4, +6, +7, +8, +9, +11, and +12. The data confirm that the three 16S rRNA regions involved—helices 18, 28, and 34—are in the direct neighborhood of the decoding area of the 30S subunit.

Keywords: 3D arrangement of rRNA; mRNA analogues; photo-crosslinking; ribosome function

INTRODUCTION

A detailed analysis of the mRNA binding site on the translating ribosome is of central importance for our understanding of the molecular mechanisms of the ribosomal function. One of the most powerful approaches for studying mRNA-rRNA contacts within the ribosome is the "site-directed crosslinking" technique (e.g., Banghu & Wollenzien, 1992; Dontsova et al., 1992). In our own experiments using this type of methodology (Dontsova et al., 1991, 1992; Rinke-Appel et al., 1993, 1994), two or three 4-thiouridine ("thioU") residues were inserted into mRNA analogues at selected positions either upstream or downstream of the AUG initiator codon, and—after binding to *Escherichia coli* ribosomes and photo-activation—the sites of crosslinking to the 16S rRNA were analyzed. In this way, a complete scan was made of all mRNA positions from −8 (in the upstream region) to +16 (in the downstream region). Different sets of mRNA sequences were used to demonstrate the independence of the crosslink sites upon the individual mRNA sequence, and the properties of the crosslinks were studied in different ribosomal complexes representing both initiation and pre- and posttranslocational states.

Although thioU can generate crosslinks with rRNA residues in high yield, the chance of crosslink formation depends very much on the mutual orientation of the thioU residue and its rRNA target residue (Favre, 1990). Thus, the use of this photoreactive nucleoside alone is unlikely to reveal more than a subset of the mRNA-rRNA contacts that are present within the ribosome. In order to broaden the spectrum of information, other photoreactive nucleoside derivatives need to be investigated and, in this paper, we describe the use of two new such compounds. The first of these is 6-thioguanosine ("thioG"), which—in the form of its corresponding triphosphate—can be incorporated directly into mRNA analogues by T7 transcription. Like thioU, thioG is a "zero-length" reagent, but, due to

Reprint requests to: Richard Brimacombe, Max-Planck-Institut für Molekulare Genetik, Ihnestrasse 73, 14195 Berlin, Germany.

different chemistry and geometry, the two nucleosides might be expected to show different crosslinking properties. The second compound that we describe here is designed to reveal neighborhoods between mRNA and rRNA bases that are not directly in contact with one another. For this purpose, mRNA analogues were prepared containing 5-methyleneaminouridine residues, again by direct T7 transcription in the presence of the corresponding nucleoside triphosphate. After transcription, the 5-methyleneaminouridine residues were derivatized by reaction with the N-hydroxy-succinimide ester of 4-(trifluoromethyl diazirino)-benzoic acid (TDB; Bochkareva et al., 1988). In the resulting derivatized uridine residues (TDB-U), the photoreactive diazirine group is at a maximum distance of 10 Å from the C5 atom in the uracil base. In contrast to the thionucleotides, TDB-U can also form crosslinks when it is in a double-helical configuration.

Our subsequent crosslinking analyses showed that, in the upstream regions of the mRNA, thioG gave similar crosslinking patterns to those found previously with thioU (Rinke-Appel et al., 1994). However, in the downstream regions, new highly specific and tRNA-dependent crosslinks were found to sites within the 16S rRNA helices 18, 28, and 34. The corresponding experiments with thioU (Dontsova et al., 1992; Rinke-Appel et al., 1993) had revealed specific crosslinks from other positions within the mRNA to different sites within the same regions of the 16S rRNA, viz. helix 34, helix 18, and the single-stranded region immediately adjacent to helix 28, and it was this set of downstream crosslinks that served to demonstrate that the earlier models for the three-dimensional folding of the 16S rRNA (Brimacombe et al., 1988; Stern et al., 1988) were seriously in error. With the new data from thioG and TDB-U, it is now possible to orient the three 16S rRNA regions—helices 18, 28, and 34—both relative to the mRNA and to each other, and the data have played an important role in the derivation of a revised model for the folding of the 16S molecule. This model, which will be presented in detail elsewhere (F. Mueller & R. Brimacombe, submitted for publ.; F. Mueller, H. Stark, M. van Heel, J. Rinke-Appel, N. Jünke, & R. Brimacombe, submitted for publ.), suggests that the incoming (downstream) mRNA passes through a hole at the head-body junction of the 30S subunit, giving a situation that is reminiscent of the "clamp" structures that have been observed in RNA- or DNA-polymerases (e.g., Jacobo-Molina et al., 1993; Polyakov et al., 1995; Herendeen & Kelly, 1996).

RESULTS

Synthesis of photoreactive nucleotides and their incorporation into mRNA

The structures of thioG, 5-methyleneaminouridine, and the resulting diazirine derivative (TDB-U) of the latter are shown in Figure 1. The triphosphates of compounds I and II are both substrates for T7 RNA polymerase, and the synthesis of the respective triphosphates is described in Materials and Methods. Figure 2 lists the sequences of the mRNA analogues containing the modified nucleotides that were used in the crosslinking studies. The upper block of sequences (G4–G9,14) are all related to the cro-mRNA from λ phage (Dontsova et al., 1991), and were transcribed from suitable DNA templates (cf. Dontsova et al., 1992) in the presence of the triphosphate of thioG. These mRNA sequences are named according to the positions of G residues in the sequence that are downstream from the AUG codon (the A residue of the latter being denoted as position +1). Thus, mRNA G5,10 contains thioG residues at positions +5 and +10, in addition to those in the upstream region. The lower block of sequences in Figure 2 were transcribed in the presence of 5-methyleneaminouridine triphosphate. The first four of these sequences are purely "synthetic" sequences, as in Dontsova et al. (1992), and are named according to the position of the U residue downstream of the AUG codon. The fifth mRNA in this block ("U-cro") is a cro-mRNA related sequence. All the mRNA sequences contain a Shine-Dalgarno sequence, separated from the AUG codon by four or six nucleotides.

The efficiency of incorporation of the modified nucleotides into the T7 RNA transcripts is lower than that of "normal" GTP or UTP. However, by varying the ratio of modified and normal UTP or GTP in the transcription mixtures, it was possible to achieve the desired level of incorporation. In each transcription, α-^{32}P-UTP was used as a source of radioactive label, and the level of incorporation of modified nucleotide was checked by digestion with ribonuclease T_2, followed by two-dimensional thin-layer chromatography. In these

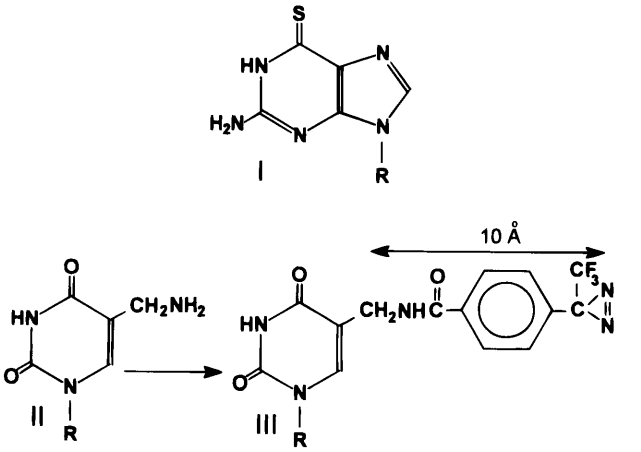

FIGURE 1. Chemical formulae of the photoreactive nucleotide bases used in this study. **I:** ThioG (6-thioguanosine). **II:** 5-Aminomethyleneuridine. **III:** TDB-U (5-aminomethyleneuridine derivatized with the N-hydroxysuccinimide ester of 4-(trifluoromethyl diazirino)-benzoic acid).

G4	GGGAAGGAGGUUGUAUGGUCAACCAACACACAC
G5,10	GGGAAGGAGGUUGUAUGAGUACUGAACACCACA
G6,11	GGGAAGGAGGUUGUAUGCUGACUCGACACCACA
G7,12	GGGAAGGAGGUUGUAUGCUCGAACUGCCACCAC
G8,13	GGGAAGGAGGUUGUAUGAUUAGCUCCGACACCA
G9,14	GGGAAGGAGGUUGUAUGAAUAAGCUCCGACACC
U5	GGGAAGGAGGAAAAAAAUGCUCGAACGGAAACGAGAG
U7	GGGAAGGAGGAAAAAAAUGGAAUACCGGAAACGACAG
U9	GGGAAGGAGGAAAAAAAUGGAAGAUCGGAAACGACAG
U11	GGGAAGGAGGAAAAAAAUGGAACGGAUAGAACGACAG
U-cro	GGGAAGGAGGUUGUAUGUAACAAUGCAAACGACAG

FIGURE 2. mRNA sequences used in this study. The AUG initiator codon and Shine-Dalgarno sequence are underlined in each case. **G** or **U** denote residues that were incorporated into the T7 transcripts using a mixture of GTP (or UTP) and the corresponding modified nucleotide (see Fig. 1). mRNA sequences are named (on the left) according to the type of photoreactive nucleotide (G for mRNAs carrying thioG residues; U for those carrying TDB-U residues), and the positions of the latter in the sequence downstream from the AUG codon (see text for details). In the thioG-containing mRNAs and the mRNA U-cro, the sequence upstream of the AUG codon is that of the cro-protein from lambda phage (Dontsova et al., 1991).

chromatograms, mononucleotides that were located on the 5′-adjacent side of a radioactive U residue appear as labeled nucleoside 3′-phosphates. An example, in the case of mRNA G7,12 (Fig. 2), is illustrated in Figure 3. Figure 3A is the T_2-digest from nonmodified mRNA, showing spots corresponding to Ap, Cp, Gp, and Up (marked 1–4, respectively). The sample in Figure 3B was transcribed in the presence of thioG triphosphate (without normal GTP), and shows the absence of Gp (spot 3) and the appearance of thioGp (spot 5). In Figure 3C, equal amounts of thioG triphosphate and GTP were included in the transcription mixture, and it can be seen that the ratio of thioGp (spot 5) to Gp (spot 3) is about 1:10. The ratio was quantified by scratching the appropriate spots from the thin-layer plate and measuring their radioactivity. Because the mRNA sequences (Fig. 2) contain 10 G residues, this ratio indicates that statistically one G residue per molecule is substituted by thioG, which is an appropriate level for the crosslinking experiments. The corresponding incorporation of 5-methyleneaminouridine was checked using mRNA U-cro (Fig. 2); here, a twofold excess of the modified UTP was added to the transcription mixtures, to give a 1:1 ratio of modified to unmodified uridine residues. For mRNAs U5–U11, this represents a statistical incorporation of one modified residue per molecule, or three modified residues in the case of mRNA U-cro. The modified uridine residues were derivatized after isolation of the mRNA transcript by reaction with the N-hydroxysuccinimide ester of TDB, according to the procedure of Bochkarev and Kogon (1992). The yield of this modification reaction was also determined by T_2 digestion and thin-layer chromatography, and was approximately 80% (data not shown). In these chromatograms, only the mobility of the 5-methyleneaminouridine spot was changed after the modification reaction, confirming that the N-hydroxysuccinimide ester of TDB reacts—as expected—specifically with the primary aliphatic amino group, and not with nucleotide bases (cf. Rinke-Appel et al., 1995).

Preparation and isolation of crosslinked complexes

^{32}P-labeled mRNA analogues containing thioG or TDB-U (Fig. 2) were bound to *E. coli* ribosomes in the

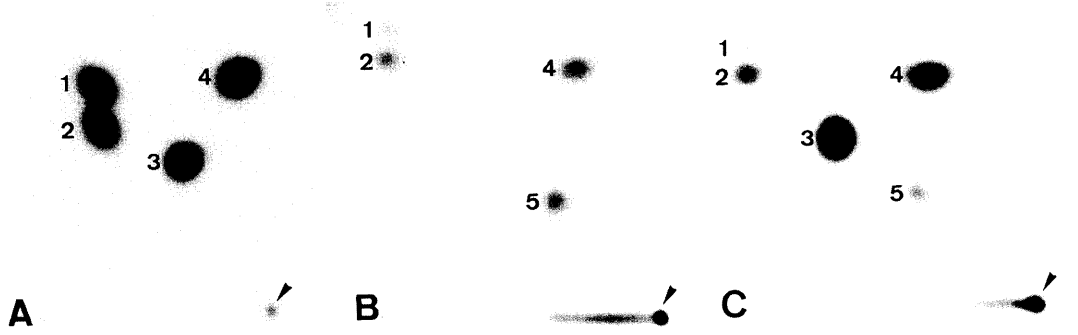

FIGURE 3. Ribonuclease T_2 fingerprints of ^{32}P-labeled mRNA G7,12 (Fig. 2), containing different amounts of thioG. The mRNA was transcribed in the presence of (**A**) normal GTP, (**B**) thioGTP, and (**C**) a 1:1 mixture of GTP and thioGTP. Numbered spots correspond to: 1, Ap; 2, Cp; 3, Gp; 4, Up; 5, thioGp. Directions of chromatography were from right to left (first dimension), and from bottom to top (second dimension). The sample application point is indicated by an arrowhead in each case.

presence or absence of initiator $tRNA_f^{Met}$ as described previously (Dontsova et al., 1991, 1992), and crosslinking of the photoreactive residues was induced by mild UV-irradiation at 350 nm (Tate et al., 1990; Bochkarev & Kogon, 1992). Control experiments showed that the crosslinking reaction was UV light-dependent; no crosslinking was observed in the absence of the irradiation step, or with mRNAs that did not contain the photoreactive nucleotides. The crosslinked 16S rRNA was isolated by two successive sucrose gradient centrifugations, the first at low magnesium concentration so as to separate the ribosomal subunits, and the second in the presence of SDS to dissociate the crosslinked 30S subunits into RNA and protein fractions. In the case of the thioG-containing mRNAs, the yield of crosslinking to 16S rRNA represented about 10–15% of the ribosome-bound mRNA, whereas with the TDB-U mRNAs, the corresponding figure was about 1%. The latter value is typical for diazirine derivatives, where the highly reactive carbene generated by the photo-activation process reacts to a large extent with the solvent (cf. Doering et al., 1994). Crosslinks to ribosomal protein are not considered in this study, because preliminary experiments showed that the protein crosslinking patterns were similar to those observed previously with the thioU-containing mRNA analogues (Dontsova et al., 1991).

In order to localize the crosslink sites on the 16S rRNA, the 16S rRNA–mRNA crosslinked complexes were first "scanned" by a series of digestions with ribonuclease H in the presence of pairs of oligodeoxynucleotides (10- or 17-mers) complementary to regions of the 16S sequence separated by 100–200 nt (Dontsova et al., 1991, 1992); in these analyses, the crosslinked ^{32}P-labeled mRNA is released as a small radioactive fragment if the two oligodeoxynucleotides concerned have "straddled" a crosslink site. Crosslinked 16S rRNA regions identified in this manner were narrowed down as far as possible by further ribonuclease H digestions in the presence of other oligodeoxynucleotides, and the precise sites of crosslinking within these regions were analyzed by primer extension (Moazed et al., 1986). Because the latter method is very prone to show artifacts when applied to the analysis of crosslinked samples (see Brimacombe, 1995, for a discussion of this point), primer extension "stop signals" were only considered as indicating a crosslink if they occurred reproducibly within the short rRNA regions already defined by the ribonuclease H digestions. In all cases, the control for the primer extension reaction was the corresponding noncrosslinked RNA fragment from the same ribonuclease H gel that was used to isolate the crosslinked fragment (see legends to Figs. 4–6, below); the crosslinked fragment runs more slowly in the gel due to the presence of the mRNA sequence. Thus, the control fragments underwent precisely the same treatment with regard to irradiation, digestion etc., as did the crosslinked fragments. The photoreactive residue within the mRNA that was involved in each crosslink was determined by ribonuclease T_1 fingerprinting of individual ribonuclease H-digested crosslinked complexes, again using our established methodology (Dontsova et al., 1992).

Crosslinks from mRNA containing thioG

The ribonuclease H analysis showed that all of the thioG-containing mRNAs tested (Fig. 2) formed a crosslink in high yield to the extreme 3′-terminal region of the 16S rRNA (nt 1530–1542). Crosslinks in lower yield were also observed to the 560–690 and 1305–1385 regions, the former being found both in the presence and absence of $tRNA_f^{Met}$ and the latter mainly in the presence of the tRNA. The ubiquitous presence of these crosslinks suggests that they arise from the G-rich upstream sequence common to all of the mRNA species, and they correspond to the crosslinks within the same 16S rRNA regions (to nt 1530, 666, and 1360, respectively) found in our previous experiments with thioU (Rinke-Appel et al., 1994). The thioU experiments had shown that crosslinks upstream of the AUG start codon were not as specific as their downstream counterparts, with respect to both tRNA dependence and precise position within the mRNA sequence. The upstream crosslinks are, consequently, not as interesting for our purpose, which is to map the precise path of the mRNA relative to the 16S rRNA and, accordingly, these crosslink sites were not analyzed in detail.

In contrast, two new crosslinks were observed with individual thioG-containing messages. One of these was formed by mRNAs G8,13 and G9,14 (Fig. 2), whereas the other was seen only with mRNA G7,12. This specificity is already a clear indication that the crosslinks concerned are from the thioG residues in the region downstream of the AUG start codon, where the individual message sequences are different, and this was confirmed in the subsequent crosslink site analyses (see below). Although in both cases the yield was relatively low (ca. 10% of the total crosslinking), the two crosslinks nonetheless were reproducibly found. Furthermore, as observed previously with crosslinks from thioU in the downstream region of the mRNA (see, e.g., Dontsova et al., 1992), crosslink formation was entirely dependent on the presence of $tRNA_f^{Met}$ (data not shown). The analysis of these crosslink sites is illustrated in Figures 4 and 5.

Figure 4 shows the analysis of the crosslink from mRNA G8,13. The preliminary ribonuclease H scan had revealed that the crosslink site lay within the 16S rRNA region 1145–1240, and Figure 4A shows the results of further ribonuclease H digestions within this RNA region, made from complexes formed with mRNA G8,13 in the presence of $tRNA_f^{Met}$. Slot 1 shows the release of a 65-nt fragment between positions 1145 and

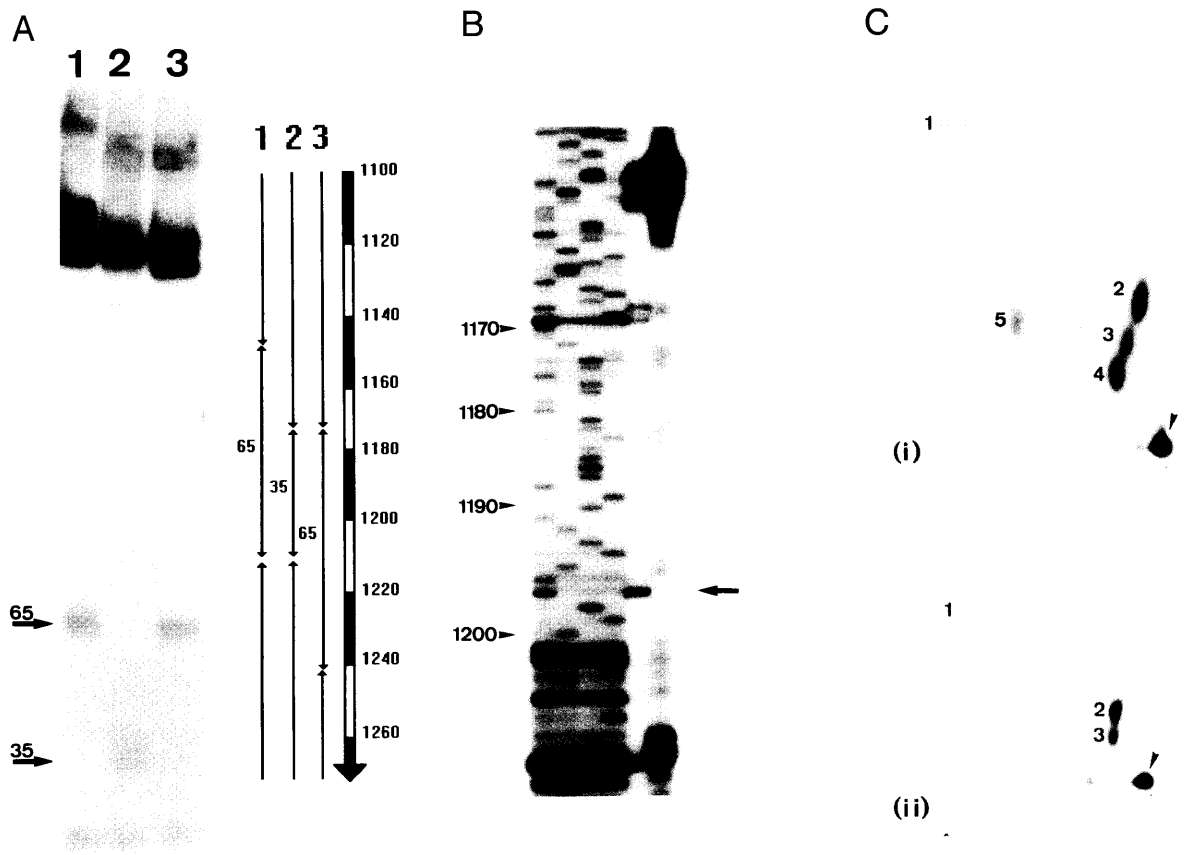

FIGURE 4. Analysis of the crosslink from mRNA position +8 to 16S rRNA nt 1196, using mRNA G8,13 (Fig. 2). **A:** Ribonuclease H digests of ^{32}P-mRNA/16S rRNA crosslinked complexes, separated by electrophoresis on a 4% polyacrylamide gel. The following pairs of oligodeoxynucleotides were used for the digestions (listed according to the position in 16S rRNA complementary to the central base of the oligodeoxynucleotide). Slot 1, positions 1145, 1210; slot 2, positions 1175, 1210; slot 3, positions 1175, 1240. The approximate sizes of the 16S fragments (linked to the ^{32}P-mRNA) excised in each case are indicated, and the locations of these fragments within the 16S sequence are summarized in the diagram on the right. **B:** Reverse transcriptase analysis of the crosslink site in 16S rRNA. Dideoxy sequencing lanes (prepared from untreated 16S rRNA) are marked A, C, G, and T, and the lanes marked X and K contained crosslinked and control samples, respectively. The crosslinked sample was a ribonuclease H-digested fragment (between 16S RNA positions 1145 and 1270), and the control sample was a similar fragment isolated from noncrosslinked 16S RNA from a parallel lane in the same gel. The primer for reverse transcription was complementary to 16S RNA positions 1226–1244. The transcription stop corresponding to the crosslink site is marked by an arrow. **C:** Ribonuclease T_1 fingerprints of (i) noncrosslinked mRNA G8,13, and (ii) mRNA G8,13 crosslinked to 16S rRNA region 1175–1210 (cf. panel A, slot 2). Directions of chromatography and sample application point are as in Figure 3. Radioactive oligonucleotide spots are: 1, Gp; 2, UUGp; 3, UAUGp; 4, AUUAGp; 5, CUCCGp (cf. mRNA sequence, Fig. 2).

1210, slot 2 a 35-nt fragment (positions 1175 and 1210), and slot 3 a 65-nt fragment (positions 1175 and 1240). The common sequence covered by these three fragments is between positions 1175 and 1210. Figure 4B gives an example of a reverse transcriptase analysis to pinpoint the crosslink site within this region; a clear stop signal can be seen in the crosslinked sample (lane X) at position 1197, corresponding to a crosslink site at position 1196. Precisely the same results were observed in the case of mRNA G9,14 (data not shown). Figure 4C shows the identification of the crosslinked nucleotide within the mRNA, by T_1 fingerprint analysis of the crosslinked complex. Figure 4C (i) is the fingerprint of free mRNA G8,13 (labeled with radioactive UTP), whereas Figure 4C (ii) is that of the isolated crosslinked complex. Spots 4 and 5, corresponding to the radioactive U-containing oligonucleotides AUUAGp and CUCCGp (cf. Fig. 2), respectively, are clearly missing from the latter fingerprint. Because a thioG residue involved in a crosslink would be expected to be resistant to T_1 digestion, this result indicates that the crosslink lies at the junction between oligonucleotides 4 and 5, i.e., at G residue 8. Again, mRNA G9,14 gave a corresponding result, indicative of a crosslink to G-9 of the mRNA.

The results of the analysis of the crosslink from mRNA G7,12 are illustrated in Figure 5. Here, the preliminary ribonuclease H scan had indicated the presence of a tRNA-dependent crosslink in the 495–580 region of the 16S rRNA. The ribonuclease H digests shown in Figure 5A indicate the release of a 55-nt fragment between positions 525 and 580 (slot 1), a similar

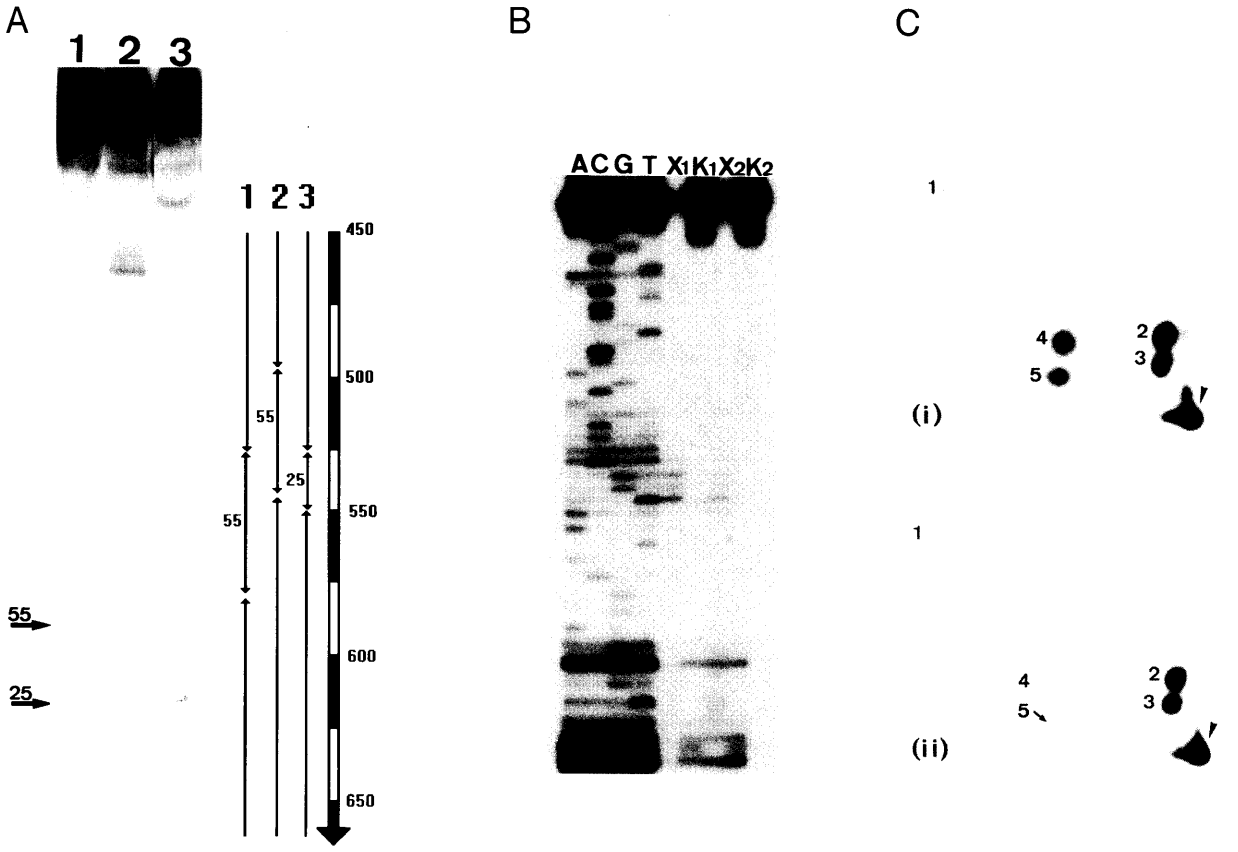

FIGURE 5. Analysis of the crosslink from mRNA position +12 to 16S rRNA nt 530, using mRNA G7,12 (Fig. 2) (cf. legend to Figure 4 for detailed description). **A:** Ribonuclease H digests of the crosslinked complex, using oligodeoxynucleotides complementary to 16S positions 525, 580 (slot 1), 490, 545 (slot 2), 525, 550 (slot 3). **B:** Reverse transcriptase analysis of the crosslink site. X_1, K_1 and X_2, K_2 are two independent sets of samples. The RNA fragment used for the analysis was a ribonuclease H-digested fragment between 16S rRNA positions 495 and 590, with a primer complementary to positions 557–584. The principal transcription stop corresponding to the crosslink site is marked by an arrow. **C:** Ribonuclease T_1 fingerprints of (i) free mRNA G7,12, and (ii) mRNA G7,12 crosslinked to 16S rRNA region 525–550 (cf. panel A, slot 3). Radioactive oligonucleotide spots are: 1, Gp; 2, UUGp; 3, UAUGp; 4, CUCGp; 5, AACUGp; the position of the latter—absent in (ii)—is indicated by an arrow (cf. mRNA sequence in Fig. 2).

55-nt fragment between positions 490 and 545 (slot 2), and a 25-nt fragment between positions 525 and 550 (slot 3); the common sequence lies between positions 525 and 545. Figure 5B shows an example of the corresponding primer extension analysis from two different crosslinked samples, both of which gave stop signals at nt 528–531 of the 16S rRNA (lanes X). This type of "stuttering" effect is quite common in reverse transcriptase analyses of crosslink sites (see Brimacombe, 1995, for discussion). Because the most predominant and reproducible stop signal was at position 531, we conclude that the crosslink site is at nt 530, although the presence of multiple sites between nt 528 and 530 cannot be excluded. The ribonuclease T_1 fingerprint analyses for mRNA G7,12 (labeled with radioactive UTP) are shown in Figure 5C. Figure 5C (i) is the fingerprint of the free mRNA, and Figure 5C (ii) is that of the crosslinked complex. In the latter fingerprint, spot 5 is entirely absent, and although—as in this example—the intensity of spot 4 was sometimes reduced, only the absence of spot 5 was reproducible. We therefore conclude that residue G12 of the mRNA is the site of crosslinking. [It should be noted that the oligonucleotide 3′ to G12, namely CCACCAC (Fig. 2), does not contain a radioactive U residue and, as a result, is not visible in the fingerprints.]

Crosslinks from mRNA containing TDB-U

The ribonuclease H analysis of the crosslinks from all the mRNA analogues containing TDB-U (Fig. 2) showed a crosslink in relatively high yield to the 16S rRNA region 920–1055, and a second crosslink in lower yield to the extreme 3′-terminal region. The latter crosslink was not dependent on the presence of tRNA, and, accordingly, was not analyzed further. In contrast, the 920–1055 crosslink was entirely dependent on the presence of $tRNA_f^{Met}$, and the analysis of this crosslink is

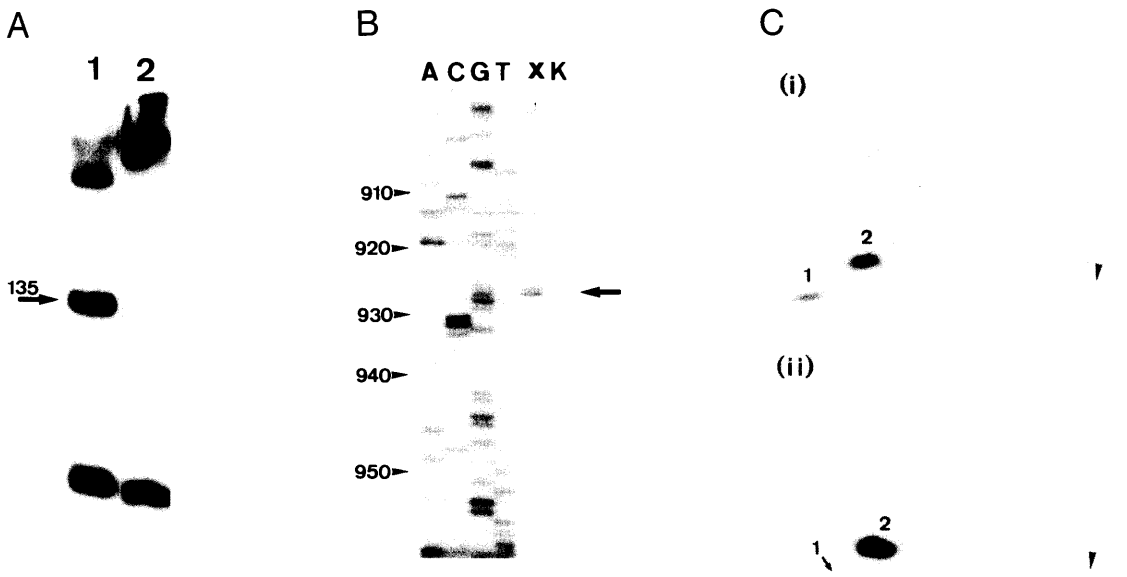

FIGURE 6. Analysis of the crosslink from mRNA position +2 to 16S rRNA nt 926, using mRNA U7 (Fig. 2) (cf. legend to Fig. 4 for detailed description). **A:** Ribonuclease digests of the crosslinked complex, using oligodeoxynucleotides complementary to 16S rRNA positions 920 and 1055. Slot 1, sample prepared in the presence of $tRNA_f^{Met}$; slot 2, sample prepared in the absence of tRNA. **B:** Reverse transcriptase analysis of the crosslink site in 16S RNA. The RNA fragment used for the analysis was a ribonuclease H-digested fragment between 16S rRNA positions 845 and 1055, and the primer was complementary to positions 996–1013. The transcription stop corresponding to the crosslink site is marked by an arrow. **C:** Ribonuclease T_1 fingerprints of (i) free mRNA U7, and (ii) mRNA U7 crosslinked to 16S rRNA region 920–945. Radioactive oligonucleotide spots are: 1, AAAAAAAUGp; 2, AAUACCGp (cf. mRNA sequence, Fig. 2).

documented in Figure 6. Figure 6A shows the result of a ribonuclease H digest in the presence (slot 1) and absence (slot 2) of $tRNA_f^{Met}$, using oligodeoxynucleotides centered on positions 920 and 1055 of the 16S rRNA; the 135-nt fragment released is only visible in the former sample. Further ribonuclease H digestions (not shown) enabled us to narrow the crosslinked region down to positions 920–945. An example of the corresponding primer extension analysis is illustrated in Figure 6B, and a prominent stop signal can be seen here at position 927. This was the only stop signal that was observed reproducibly within the crosslinked region (920–945) delineated by the ribonuclease H analysis, and indicates that the crosslink site was to position 926. [The additional stop signals that can be seen in Figure 6 between positions 910 and 920 lie outside the region identified by ribonuclease H digestion, and were not observed reproducibly. This is a typical example of the type of artifact that is observed with the primer extension method in analyses of crosslink sites, as discussed in detail by Brimacombe (1995)].

The fact that all of the TDB-U messages showed the same crosslink is of itself strongly suggestive that the crosslink site within the mRNA must be at U residue +2, this being the only U residue common to all the sequences. This is confirmed by the ribonuclease T_1 fingerprints in Figure 6C, from mRNA U7 (Fig. 2). Figure 6C (i) is the fingerprint of the free mRNA (labeled with radioactive UTP), whereas Figure 6C (ii) is that of the crosslinked complex. Despite the heavy exposure of the autoradiogram in the latter Figure, it is clear that spot 1 (AAAAAAAUGp) is almost entirely absent, indicating that the U residue within this oligonucleotide—namely U2—is the site of crosslinking in the mRNA.

DISCUSSION

All of the crosslink sites to 16S rRNA that we have identified from the downstream region of mRNA (Dontsova et al., 1992; Rinke-Appel et al., 1993; this paper) are summarized in Figure 7. The application of the new photoreactive nucleotides thioG and TDB-U described here has enabled us to analyze three new contacts between mRNA and 16S rRNA, namely from mRNA position +2 to G-926 of the 16S rRNA, from positions +8 and +9 to A-1196, and from position +12 to G-530. ThioG and thioU are both "zero-length" crosslinking reagents, and the respective positions of the thio group in the two compounds are only about 1.5 Å apart, relative to the phosphate backbone of the mRNA. However, thioU and thioG are likely to exhibit quite different photo-crosslinking mechanisms (Rackwitz & Sheit, 1974; Favre, 1990), and this is reflected in the markedly different crosslinking patterns that we have observed in the downstream region of the mRNA. Whereas with thioU crosslinks to 16S rRNA were found from positions +4, +6, +7, and +11 of the mRNA

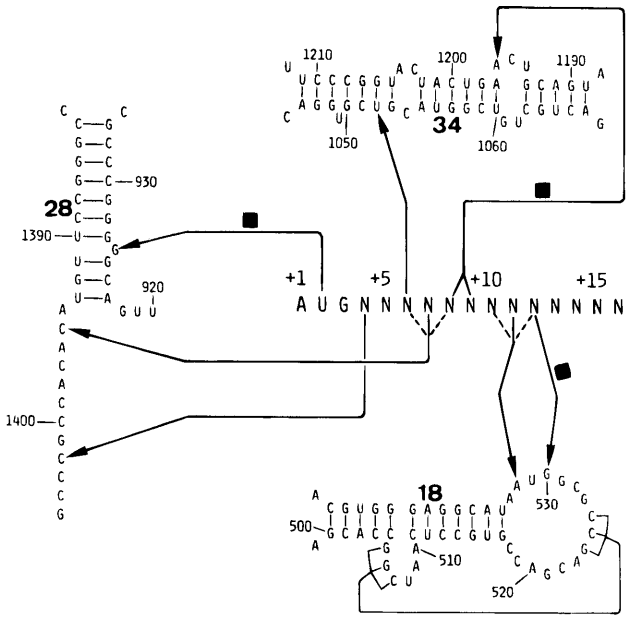

FIGURE 7. Summary of the crosslinking data from the downstream region of the mRNA. The central part of the figure shows a generalized mRNA sequence (AUGNNN.....), and the crosslink sites to 16S rRNA in the regions of helices 18, 28, and 34 are indicated. Crosslinks described in this paper are marked with black squares; the remainder are from Dontsova et al. (1992) and Rinke-Appel et al. (1993).

(Dontsova et al., 1992; Rinke-Appel et al., 1993), here we have found crosslinking with thioG from positions +8, +9, and +12. Neither thioU nor thioG are able to form crosslinks if the mRNA base concerned is involved in duplex formation. However, with TDB-U this is not the case, and, as a result, we were able for the first time to observe a crosslink from a position (+2) within the codon-anticodon duplex of P-site bound tRNA. The 5-methyleneamino group is situated in the major groove of the RNA helix, and the 10-Å bridging distance of the TDB-U derivative is sufficient to make contact with the rRNA.

Taken together, the data (Fig. 7) now define contacts to 16S rRNA from positions +2, +4, +6, +7, +8, +9, +10, +11, and +12 of the mRNA. These contacts involve three distinct regions of the 16S rRNA (helices 18, 28, and 34) and provide conclusive evidence that these regions are in the direct neighborhood of the decoding area of the 30S subunit. In addition to the crosslink sites to mRNA, the loop-end of helix 18 is known to contain footprint sites to tRNA bound at the A-site in the presence of poly (U) (Moazed & Noller, 1990), sites where mutation causes resistance to streptomycin (Powers & Noller, 1991), and a site involved in termination of translation (Shen & Fox, 1989). Similarly, in helix 34, the mRNA crosslink site to nt 1052 (Fig. 7) is close to the translational suppressor site at 1054 (Murgola et al., 1988), and the corresponding mRNA site at 1196 is close to the site (1192) where mutation causes resistance to spectinomycin (Sigmund et al., 1984). In helix 28, the nucleotide (G-926) that is crosslinked to mRNA position +2 is universally conserved, and has been shown to be essential for P-site tRNA binding (Von Ahsen & Noller, 1995). The immediately adjacent single-stranded region (1394–1408) contains the mRNA crosslink sites from positions +4 and +7 (Fig. 7), as well as footprint sites for A- and P-site bound tRNA in the presence of mRNA (Moazed & Noller, 1990) and the crosslink site from position 34 of the P site tRNA to C-1400 of the 16S rRNA (Prince et al., 1982).

As noted in the Introduction, the mRNA crosslinking data have been incorporated into a revised model for the three-dimensional arrangement of the 16S rRNA. In this model, the three 16S rRNA regions—helices 18, 28, and 34—are closely juxtaposed to the decoding area of the 30S subunit, in contrast to their locations in the earlier models (Brimacombe et al., 1988; Stern et al., 1988). The new model also satisfies a large amount of other new topographical information, and will be described in detail elsewhere (F. Mueller & R. Brimacombe, submitted for publ.; F. Mueller, H. Stark, M. van Heel, J. Rinke-Appel, N. Jünke, & R. Brimacombe, submitted for publ.). However, some general aspects of the model should be mentioned here, which are relevant to the question of the path of the mRNA through the 30S subunit.

An important feature of the new 16S model is that the rRNA has been fitted to an electron microscopic reconstruction at 19-Å resolution of the *E. coli* 70S ribosome (Stark et al., 1997), in which the A and P site tRNAs were directly visible. This latter observation effectively pinpoints the location of the decoding region within the 30S subunit, and at the same time imposes a set of stringent additional constraints on the folding of the 16S rRNA, particularly in light of a recent set of site-directed crosslinking data between the 16S rRNA and tRNA located at the ribosomal A, P, or E sites (Rinke-Appel et al., 1995). In the 70S electron microscopic reconstruction, the A and P site tRNA molecules are in the "S" configuration (Lim et al., 1992) relative to one another, in an arrangement that is essentially very similar to that proposed by Wower et al. (1989). In this arrangement, the anticodon stem-loops of the A and P site tRNA molecules lie interposed between the mRNA and the head of the 30S subunit, a fact that would appear to contradict our observation of zero-length crosslinks from positions within or close to the mRNA A site codon to helix 34; helix 34 is unequivocally located in the head of the subunit in all the published models for the three-dimensional organization of the 16S rRNA (e.g., Brimacombe et al., 1988; Stern et al., 1988). However, in our previous studies with thioU (Dontsova et al., 1992; Rinke-Appel et al., 1993), we had observed that the mRNA crosslinks from positions +4, +6, and +7 (in the region of the A site codon)

were only formed in the presence of tRNA at the P site, and were strongly inhibited by a concomitantly bound A site tRNA. This clearly implies that the cross-linked nucleotides (particularly those in helix 34) can only come into close contact with the corresponding sites on the mRNA (cf. Fig. 7) in the absence of an A site tRNA. Whether this is achieved by movement of the mRNA, or of helix 34, or both, remains to be seen, but the conclusion is nevertheless that a detailed interpretation of the data cannot be made in terms of a static model for the mRNA-rRNA interaction (see Brimacombe, 1995, for discussion of this point).

A further aspect of the electron microscopic reconstruction of the 70S ribosome (Stark et al., 1997) mentioned above is that there is a "hole" in the 30S subunit at the head-body junction. This feature was also observed in earlier electron microscopic reconstructions (Frank et al., 1995; Stark et al., 1995), and it has been proposed that the incoming mRNA passes through this hole (Frank et al., 1995). The positions of the tRNA molecules in the latter publications were only deduced, as opposed to being visualized directly as in Stark et al. (1997), but this newer reconstruction—combined with the locations in the revised 16S rRNA model for helices 18, 28, and 34—supports the proposed mRNA path through the hole. There is, in fact, only one covalent link between the head and the body of the 30S subunit (namely helix 28; Brimacombe et al., 1988; Stern et al., 1988), and the hole can be described more properly as being the result of a second (noncovalent) contact between the two domains of the subunit (Stark et al., 1995). The initial contact between an mRNA molecule and the ribosome is the formation of the Shine-Dalgarno interaction with the upstream region of the mRNA, and it seems highly unlikely that—prior to forming the Shine-Dalgarno interaction—the mRNA should have to thread its way through a hole in the 30S subunit. We therefore suggest—speculatively—that the second (noncovalent) head-body contact is able to open and close in a manner analogous to the clamp or ring structures that have been observed in DNA polymerase III (Herendeen & Kelly, 1996), *E. coli* core RNA polymerase (Polyakov et al., 1995), and reverse transcriptase (Jacobo-Molina et al., 1993). Thus, the mRNA could form the Shine-Dalgarno interaction in the "open" phase, and the head-body junction would then close, clamping the mRNA into position. Such a mechanism would ensure that the mRNA is positioned correctly as it approaches the decoding area, and is consistent with the concept of a "stand-by" site for the mRNA (Canonaco et al., 1989; La Teana et al., 1995), whereby the mRNA becomes relocated partially under the influence of the initiation factors. A similar conclusion has been reached very recently by Lata et al. (1996).

MATERIALS AND METHODS

Synthesis of modified nucleoside triphosphates

Except where noted, reagents were obtained commercially and used without further purification. 6-Mercaptoguanosine was obtained from Sigma, 5-methyluridine from Aldrich, DEAE-cellulose DE-52 from Whatman, Dowex 50 WX2 (200–400 mesh) from Serva, and silica gel for column chromatography (230–400 mesh) from Merck. Dimethyl formamide (DMF) was dried by distillation over CaH_2 under reduced pressure and was stored over 4A molecular sieves. Pyridine was distilled four times over P_2O_5, *p*-toluenesulphonyl chloride, and NaOH, and stored over 4A molecular sieves. Triethyl phosphate was distilled over CaH_2 under reduced pressure and stored over CaH_2. Tributylamine was distilled twice over NaOH under reduced pressure. Methylimidazole was dried over 4A molecular sieves. Toluene and dichloroethane were distilled over P_2O_5. Dioxane was distilled over NaOH. Ethyltrifluoroacetate was obtained by reacting trifluoroacetic acid with ethanol in the presence of P_2O_5, followed by distillation. An anhydrous 0.5 M solution of tris-(tri-*n*-butylammonium)-pyrophosphate was prepared as follows. Sodium pyrophosphate decahydrate (2.23 g, 5 mmol) was dissolved in water and applied to a Dowex H^+ column. Pyrophosphoric acid was eluted with water and collected in an ice-cooled flask. Tri-*n*-butylamine (3.65 mL, 15 mmol) was added, the mixture was shaken, and then evaporated in vacuo. The oil obtained was evaporated four times with anhydrous pyridine and then dissolved in 10 mL of anhydrous DMF.

The ^1H, ^{31}P, and ^{13}C NMR spectra (200.132 MHz, 81.015 MHz, and 50.323 MHz, respectively) were recorded using a Bruker AC 200 spectrometer. Absorption spectra were measured on a Karl Zeiss Specord UV-VIS instrument. Analytical thin-layer chromatography was conducted on silica gel plates (Merck, Kieselgel 60 F254). HPLC purifications were performed using a Waters 600 E instrument equipped with a multisolvent delivery system and a model 484 tunable absorbence detector. Lichroprep RP-18 (15–25 mkm, Merck) was used as matrix for reverse-phase chromatography. Yields of all products and intermediates were determined spectrophotometrically. NMR spectra were not recorded for the intermediate compounds.

Synthesis of thioG 5′-triphosphate

6-Mercaptoguanosine (50 mg, 0.162 mmol) was evaporated three times with anhydrous pyridine, dissolved with heating in triethylphosphate (0.5 mL), and cooled on ice. $POCl_3$ (0.194 mmol) was added, and the mixture incubated for 8 min on ice. Next, 0.5 M tris-(tri-*n*-butylammonium)-pyrophosphate (2 mL) and tributylamine (0.24 mL) were added, stirred for 3 min, and mixed with 1 M triethylammonium bicarbonate (10 mL), followed by evaporation in vacuo. The thioG triphosphate was dissolved in water (200 mL) and applied to a DEAE-cellulose DE-52 column (1.5 × 24 cm). The column was eluted with a linear gradient (0.5 L) of triethylammonium bicarbonate, pH 7.5 (0.0–0.3 M). Fractions containing the product were pooled, evaporated, dissolved in water, and applied to a Lichrosorb RP-18 column (1 × 25 cm). The product was eluted using a linear gradient

of acetonitrile (0–10%) in 0.05 M triethylammonium bicarbonate, pH 7.5. Solvent was removed on a rotary evaporator, and the thioG triphosphate was evaporated three times with ethanol, giving a yield of 0.08 mmol (50%). The product had an R_f of 0.1 in dioxane:NH_4OH:H_2O (6:1:4 v/v), and exhibited a characteristic UV spectrum ($\epsilon = 2.48 \times 10^4$ at 342 nm in aqueous solution, pH 4.5). The NMR spectrum of the product was as follows. ^1H NMR: δ = 1.29 (t,J = 8 Hz, CH_3 of $(C_2H_5)_3NH^+$, 22H), 3.1 (q,J = 8 Hz, CH_2 of $(C_2H_5)_3NH^+$, 15H), 4.26 (m, br.s, H5′, 2H), 4.4 (m.br.s H4′, 1H), 4.65 (m.br.s, H3′, 1H), 4.75 (m.br.s, H2′, 1H), 5.95 (d,J = 6 Hz, H1′, 1H), 8.31 (s, H8, 1H); ^{13}C NMR (D_2O) δ = 11.2 (CH_3 of $(C_2H_5)_3NH^+$), 42.8 (CH_2 of $(C_2H_5)_3NH^+$), 65.9 (C5′), 71.0 (C2′), 74.3 (C3′), 84.7 (C4′), 87.8 (C1′), 129.1 (C1), 141.2 (C2 and C8), 148.9 (C4), 154.4 (C6); ^{31}P NMR (D_20) δ = 22.56 (t,J = 25 Hz, P_β, 1P), −11.17 (d,J = 25 Hz, P_α, 1P), −8.13 (d,J = 25 Hz, P_γ, 1P).

Synthesis of 5-aminomethyleneuridine 5′-triphosphate

2′, 3′, 5′-Triacetyl 5-methyluridine

5-Methyluridine (153 mg) was evaporated three times with anhydrous pyridine (5 mL), dissolved in pyridine (2 mL), and acetic anhydride (0.46 mL) and methylimidazole (100 μL) were added. After 5 min, the pyridine was removed by rotary evaporation and the residue was evaporated three times with toluene. The oily material obtained was dissolved in the minimum volume of chloroform and applied to a silica gel column (0.5 × 8.5 cm). The product was purified using a linear gradient of ethanol (0–10%) in chloroform. Fractions containing the product were pooled, evaporated, and dried over P_2O_5 in vacuo. The product (yield 95%) had an R_f of 0.8 in ethanol:chloroform (1:4, v/v).

2′, 3′, 5′-triacetyl 5-bromomethyleneuridine

Triacetyl 5-methyluridine from the previous step was dissolved in freshly distilled 1,2-dichloroethane (9.7 mL), and placed in a three-neck flask equipped with a condenser and dropping funnel. The subsequent reaction proceeded under intensive illumination with a powerful tungsten lamp, in an argon atmosphere; after the mixture began to boil, a solution of bromine (47 μL) in dichloroethane (2.3 mL) was added dropwise over a period of 3 h. The reaction mixture was then cooled and evaporated, and the oil obtained was washed with toluene (200 μL) and redissolved in dichloroethane. The product was precipitated by adding the solution dropwise into hexane. The precipitate was collected and dried, the product (yield 80%) having an R_f of 0.65 in ethyl acetate: hexane (4:1, v/v).

5-Aminomethyleneuridine

The triacetyl 5-bromomethylene uridine from the previous step was dissolved in dioxane saturated with dry NH_3 (830 μL), and NH_3, dried by blowing through a tube containing granulated NaOH, was bubbled through the reaction mixture for 2 h. The resulting precipitate was filtered off, the solvent removed by rotary evaporation, and the residue was treated with concentrated aqueous ammonia overnight. After evaporation of the ammonia, the residue was dissolved in water and applied to a Dowex 50 (H^+) column, which was washed successively with water, 30% ethanol, and 2% (wt) ammonia in 30% ethanol. The product was eluted at the third step. After evaporation of the fractions containing the product, the final purification was achieved by HPLC on a Lichroprep RP-18 column (1 × 25 cm) using a linear gradient of methanol (0–50%) in water. Solvent was removed by rotary evaporation, and the product (yield 55%) dried over P_2O_5 in vacuo; the product gave an R_f of 0.2 in NH_4OH:methanol (5:95, v/v).

5-(N-trifluoroacetyl)-aminomethyleneuridine

The 5-aminomethyleneuridine obtained in the previous step was dissolved in methanol with heating, ethyltrifluoroacetate (2 mL) was added, and the pH of the solution was adjusted to 8 by addition of methylimidazole. The reaction was allowed to proceed for 5 days at room temperature. The reaction mixture was then evaporated, dissolved in the minimum volume of chloroform, and applied to a silica gel column (0.5 × 8.5 cm). The column was eluted with a linear gradient of ethanol (0–20%) in chloroform (1 L). Fractions containing the product were pooled and evaporated, the product (yield 60%) having an R_f of 0.4 in methanol:chloroform (1:3, v/v).

5-Aminomethyleneuridine 5′-triphosphate

5-(N-trifluoroacetyl)-aminomethyleneuridine (0.187 mmol) from the previous step was evaporated four times with acetone, and dried over P_2O_5 in vacuo. Phosphorylation was performed as described for thioG 5′-triphosphate (see above). After the chromatography on the DEAE-cellulose column, fractions containing the product were treated with concentrated aqueous ammonia overnight at room temperature to remove the protecting groups, and the ammonia was removed by rotary evaporation. Final purification of the product was completed using a Lichroprep RP-18 column, again as described for thioG 5′-triphosphate (above). Fractions containing the product were evaporated, and the residue dissolved in the minimum volume of water, followed by precipitation with 2% $LiClO_4$ in acetone. The pellet was washed with acetone and dried in vacuo. The product (yield 55%) gave an R_f of 0.05 in dioxane:NH_4OH:water (6:1:4, v/v). The product showed a UV spectrum in water with molar extinction values ϵ_{208}, e_{266} = 6,300; ϵ_{233} = 1,200. The observed NMR spectra were as follows. ^1HNMR (D_2O) δ = 4.03 (s, CH_2, 2H), 4.32 (m, bs, H4′, H5′, 3H), 4.44 (m, bs, H2′, H3′, 2H), 6.00 (d,J = 7.5 Hz, H1′, 1H), 8.37 (s, H6, 1H); ^{13}C NMR (D_2O) δ = 36.4 (CH_2), 65.0 (C5′), 69.8 (C2′), 75.0 (C3′), 83.9 (C4′), 89.6 (C1′), 107.6 (C5), 142.8 (C6), 152.4 (C2), 165.5 (C4); ^{31}P NMR (D_2O) δ = 19.36 (t,J = 24 Hz, P_β, 1P), −9.42 (d,J = 24 Hz, P_α, 1P), −4.22 (d,J = 24 Hz, P_γ, 1P).

Preparation of ^{32}P-labeled mRNA analogues, formation of ribosomal complexes, and analysis of crosslink sites

mRNA analogues were prepared by T7 transcription in the presence of α-^{32}P-UTP from synthetic DNA templates ac-

cording to our standard procedure (Stade et al., 1989; Dontsova et al., 1992). In the case of thioG, the ratio of thioGTP: GTP in the reaction mixtures was 1:1, in order to give a ratio of incorporation of thioG:G of 1:10 (see text and Fig. 3). In the case of 5-aminomethyleneuridine, the triphosphate was added in a twofold excess over UTP, to give an incorporation ratio of 1:1 modified:normal uridine residues. mRNA analogues containing 5-aminomethyleneuridine were derivatized by reaction with the N-hydroxysuccinimide ester of TDB (Bochkareva et al., 1988; cf. Bochkarev & Kogon, 1992) under the conditions described by Mitchell et al. (1993). Levels of incorporation of modified nucleotides, and the extent of derivatization with the diazirine in the case of TDB-U, were determined by ribonuclease T_2 digestion followed by two-dimensional thin-layer chromatography as described by Stade et al. (1989). All other procedures, including formation of ribosomal complexes, crosslinking by irradiation at 350 nm, separation of 16S rRNA-mRNA crosslinked complexes by sucrose gradient centrifugation, identification of crosslink sites on 16S rRNA by ribonuclease H digestion and primer extension analysis, and determination of the crosslinked residues within the mRNA by ribonuclease T_1 fingerprinting, were performed according to our published procedures (Dontsova et al., 1991, 1992).

ACKNOWLEDGMENTS

We are most grateful to Dr. Dmitry Bochkariov for the gift of the diazirine reagent. This work was supported in part by grants from the Russian Foundation for Basic Research, and from NATO (CRG 920349).

Received December 2, 1996; returned for revision January 15, 1997; revised manuscript received February 12, 1997

REFERENCES

Bhangu R, Wollenzien P. 1992. Binding track in the *E. coli* ribosome for mRNAs of different sequences. *Biochemistry 31*:5937–5944.

Bochkarev D, Kogon A. 1992. Application of 3-[3-(3-(tri-fluoromethyl)-diazirin-3-yl)-phenyl] 2,3-dihydroxypropionic acid; carbene generating, cleavable crosslinking agent for photo-affinity labelling. *Anal Biochem 204*:90–95.

Bochkareva ES, Lissin NM, Girshovich AS. 1988. Transient association of newly synthesized unfolded proteins with the heat-shock GroEL protein. *Nature 336*:254–257.

Brimacombe R. 1995. The structure of ribosomal RNA: A three-dimensional jigsaw puzzle. *Eur J Biochem 230*:365–383.

Brimacombe R, Atmadja J, Stiege W, Schüler D. 1988. A detailed model of the three-dimensional structure of *E. coli* 16S ribosomal RNA in situ in the 30S subunit. *J Mol Biol 199*:115–136.

Canonaco MA, Gualerzi CO, Pon CL. 1989. Alternative occupancy of a dual ribosomal binding site by mRNA affected by translational initiation factors. *Eur J Biochem 182*:501–506.

Doering T, Mitchell P, Osswald M, Bochkariov D, Brimacombe R. 1994. The decoding region of 16S RNA; a cross-linking study of the ribosomal A, P and E sites using tRNA derivatized at position 32 in the anticodon loop. *EMBO J 13*:2677–2685.

Dontsova O, Dokudovskaya S, Kopylov A, Bogdanov A, Rinke-Appel J, Jünke N, Brimacombe R. 1992. Three widely-separated positions in the 16S RNA lie in or close to the ribosomal decoding region: A site-directed cross-linking study with mRNA analogues. *EMBO J 11*:3105–3116.

Dontsova OA, Kopylov AM, Brimacombe R. 1991. The location of mRNA in the ribosomal 30S initiation complex: Site-directed cross-linking of mRNA analogues carrying several photo-reactive labels simultaneously on either side of the AUG start codon. *EMBO J 10*:2613–2620.

Favre A. 1990. 4-Thiouridine as an intrinsic photoaffinity probe of nucleic acid structure and interactions. In: Morrison H, ed. *Bioorganic photochemistry: Photochemistry and the nucleic acids, V1*. New York: Wiley Inc. pp 380–420.

Frank J, Zhu J, Penczek P, Li Y, Srivastava S, Verschoor A, Radermacher M, Grassucci R, Lata RK, Agrawal RK. 1995. A model of protein synthesis based on cryo-electron microscopy of the *E. coli* ribosome. *Nature 376*:441–444.

Herendeen DR, Kelly TJ. 1996. DNA polymerase III: Running rings around the fork. *Cell 84*:5–8.

Jacobo-Molina A, Ding JP, Nanni RG, Clark AD, Lu X, Tantillo C, Williams RL, Kamer G, Ferris AL, Clark P, Hizi A, Hughes SH, Arnold E. 1993. Crystal structure of human immunodeficiency virus type I reverse transcriptase complexed with double-stranded DNA at 3.0 Å resolution shows bent DNA. *Proc Natl Acad Sci USA 90*:6320–6324.

Lata KR, Agrawal RK, Penczek P, Grassucci R, Zhu J, Frank J. 1996. Three-dimensional reconstruction of the *E. coli* 30S ribosomal subunit in ice. *J Mol Biol 262*:43–52.

La Teana A, Gualerzi CO, Brimacombe R. 1995. From stand-by to decoding site. Adjustment of the mRNA on the 30S ribosomal subunit under the influence of the initiation factors. *RNA 1*:772–782.

Lim V, Venclovas C, Spirin A, Brimacombe R, Mitchell P, Mueller F. 1992. How are tRNAs and mRNA arranged in the ribosome? An attempt to correlate the stereochemistry of the tRNA-mRNA interaction with constraints imposed by the ribosomal topography. *Nucleic Acids Res 20*:2627–2637.

Mitchell P, Stade K, Osswald M, Brimacombe R. 1993. Site-directed cross-linking studies on the *E. coli* tRNA-ribosome complex; determination of sites labelled with an aromatic azide attached to the variable loop or aminoacyl group of tRNA. *Nucleic Acids Res 21*:887–896.

Moazed D, Noller HF. 1990. Binding of tRNA to the ribosomal A and P sites protects two distinct sets of nucleotides in 16S rRNA. *J Mol Biol 211*:135–145.

Moazed D, Stern S, Noller HF. 1986. Rapid chemical probing of conformation in 16S ribosomal RNA and 30S subunits using primer extension. *J Mol Biol 187*:399–416.

Murgola EJ, Hijazi KA, Göringer U, Dahlberg AE. 1988. Mutant 16S ribosomal RNA: A codon-specific translational suppressor. *Proc Natl Acad Sci USA 85*:4162–4165.

Polyakov A, Severinova E, Darst SA. 1995. Three-dimensional structure of *E. coli* core polymerase: Promoter binding and elongation conformations of the enzyme. *Cell 83*:365–373.

Powers T, Noller HF. 1991. A functional pseudoknot in 16S ribosomal RNA. *EMBO J 10*:2203–2214.

Prince JB, Taylor BH, Thurlow DL, Ofengand J, Zimmermann RA. 1982. Covalent cross-linking of $tRNA^{Val}$ to 16S RNA at the ribosomal P site; identification of cross-linked residues. *Proc Natl Acad Sci USA 79*:5450–5454.

Rackwitz H, Sheit K. 1974. Die Synthese von Purinnucleosid-6-Sulfonaten. *Chem Ber 107*:2284–2294.

Rinke-Appel J, Jünke N, Brimacombe R, Lavrik I, Dokudovskaya S, Dontsova O, Bogdanov A. 1994. Contacts between 16S ribosomal RNA and mRNA, within the spacer region separating the AUG initiator codon and the Shine-Dalgarno sequence; a site-directed cross-linking study. *Nucleic Acids Res 22*:3018–3025.

Rinke-Appel J, Jünke N, Dokudovskaya S, Dontsova O, Bogdanov A, Brimacombe R. 1993. Site directed cross-linking of mRNA analogues to 16S ribosomal RNA; a complete scan of crosslinks from all positions between +1 and +16 on the mRNA, downstream from the decoding site. *Nucleic Acids Res 21*:2853–2859.

Rinke-Appel J, Jünke N, Osswald M, Brimacombe R. 1995. The ribosomal environment of tRNA: Crosslinks to rRNA from positions 8 and 20:1 in the central fold of tRNA located at the A, P, or E site. *RNA 1*:1018–1028.

Shen Z, Fox TD. 1989. Substitution of an invariant nucleotide at the base of the highly-conserved 530-loop of 15S rRNA causes suppression of yeast mitochondrial ochre mutations. *Nucleic Acids Res 17*:4535–4539.

Sigmund CD, Ettayebi M, Morgan EA. 1984. Antibiotic resistance mutations in 16S and 23S ribosomal RNA genes of *E. coli*. *Nucleic Acids Res 12*:4653–4663.

Stade K, Rinke-Appel J, Brimacombe R. 1989. Site-directed cross-linking of mRNA analogues to the *E. coli* ribosome; identification of 30S ribosomal components that can be cross-linked to mRNA at various points 5′ with respect to the decoding site. *Nucleic Acids Res 17*:9889–9908.

Stark H, Mueller F, Orlova EV, Schatz M, Dube P, Erdemir T, Zemlin F, Brimacombe R, Van Heel M. 1995. The 70S *E. coli* ribosome at 23 Å resolution: Fitting the ribosomal RNA. *Structure 3*:815–821.

Stark H, Orlova EV, Rinke-Appel J, Jünke N, Mueller F, Rodnina M, Wintermeyer W, Brimacombe R, Van Heel M. 1997. Arrangement of tRNAs in pre- and post-translocational ribosomes revealed by electron cryomicroscopy. *Cell 88*:19–28.

Stern S, Weiser B, Noller HF. 1988. Model for the three-dimensional folding of 16S ribosomal RNA. *J Mol Biol 204*:447–481.

Tate W, Greuer B, Brimacombe R. 1990. Codon recognition in polypeptide chain termination; site-directed cross-linking of termination codon to *E. coli* release factor 2. *Nucleic Acids Res 18*: 6537–6544

Von Ahsen U, Noller HF. 1995. Identification of bases in 16S rRNA essential for tRNA binding at the 30S ribosomal P site. *Science 267*:234–237.

Wower J, Hixson SS, Zimmermann RA. 1989. Labelling the peptidyl transference center of the *E. coli* ribosome with photoreactive $tRNA^{Phe}$ derivatives containing azidoadenosine at the 3′ end of the acceptor arm: A new model of the tRNA–ribosome complex. *Proc Natl Acad Sci USA 86*:5232–5236.